Comparison of the Pulsed Power Supply Systems Using the PFN Switching Capacitor Method and the IGBT Chopping Method for the J-PARC 3-GeV RCS Injection System

T. Takayanagi, T. Ueno, K. Horino, T. Togashi, N. Hayashi, M. Kinsho, and Y. Irie

***Abstract*—Each pulsed power supply of the bending magnets of the 3-GeV Rapid Cycling Synchrotron injection area at the Japan Proton Accelerator Research Complex has been designed and manufactured for the painting injection in the transverse plane. The magnet currents of both the shift bump magnet and the pulsed steering magnet have a shape of trapezoidal waveform, the flat-top part of which is used for beam injection. The horizontal and vertical painting bump magnets change the beam orbit by using a decaying waveform of the magnet current dynamically. The system with a pulse forming network switching capacitor produces lower current ripples due to the limited number of switchings for the waveform formations. On the other hand, the system of an Insulated Gated Bipolar Transistor chopping system cannot be free from ripple generation due to the continuous switching. However, the Insulated Gated Bipolar Transistor chopping method has an advantage, which produces any shape of required waveform. This paper summarizes the comparison of these power supply systems from view point of the switching noises.**

***Index Terms*—IGBT and J-PARC, PFN, pulsed power supply, switching noise.**

I. INTRODUCTION

THE Japan Proton Accelerator Research Complex (J-PARC) is comprised of three accelerators and three experimental facilities [1]–[3]. The 3-GeV Rapid Cycling Synchrotron (RCS) [4] is the second accelerator, which has two functions, one is a source to produce the neutron and muon at the Material and Life Science Experimental Facility (MLF) and another is an injector to the following 50-GeV Synchrotron (MR). The injected proton beam from the Linear Accelerator (LINAC) to the RCS is accelerated up to 3 GeV at 25 Hz. With the upgrading of both the injection beam energy from 181 MeV to 400 MeV and the maximum peak current increasing from 30 mA to 50 mA of LIANC, the high intensity beam power of 1 MW with painting injection is the primary goal of the RCS. For this purpose, it is important to reduce the unnecessary beam loss during the injection and acceleration periods. The continuous current ripple noise due to the switching resonates with load and excites a forced beam oscillation [5], [6]. So the reduction of the switching noise caused by switching operation to form the waveform is essential toward power upgrade.

Manuscript received July 17, 2013; accepted December 2, 2013. Date of publication December 11, 2013; date of current version December 30, 2013.

T. Takayanagi, T. Ueno, K. Horino, T. Togashi, N. Hayashi, and M. Kinsho are with the JAEA/JPARC, Ibaraki 319-1195, Japan (e-mail: tomohiro.takayanagi@j-parc.jp).

Y. Irie is with the KEK, Ibaraki 305-0801, Japan.

Digital Object Identifier 10.1109/TASC.2013.2294400

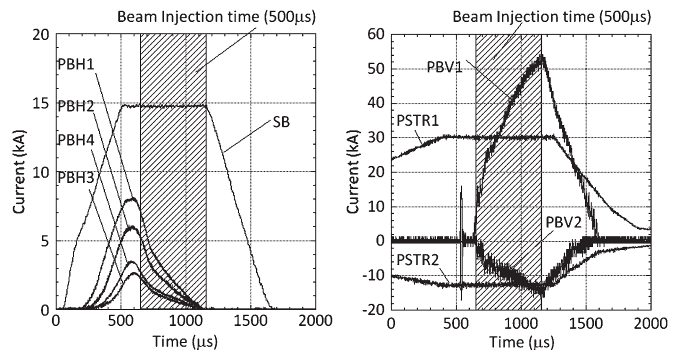

Fig. 1. Measured waveforms of each pulsed power supply at 540 kW beam power. The left graph shows the waveforms of SB and PBH. The right graph shows the waveform of PBV and PSTR. Setting parameter of the current is for MR; SB is 14.8 kA, PBH1 is 7.62 kA, PBH2 is 5.64 kA, PBH3 is 2.51 kA, PBH4 is 2.97 kA, PBV1 and PBV2 are 530 A and −137 A with correlated paintings, PSTR1 is 33.8 A and PSTR2 is −14.4 A. The formulas of the flexible current waveforms of PBH and PBV are $\mathrm{I = Imax(1 - (t/500)^{\wedge 0.5})}$ and $\mathrm{I = Imax(t/5)^{\wedge 0.5}}$, respectively. Max means a rating current of each power supply. The rating current [16]; PBH1 is 29 kA, PBH2 23.4 kA, PBH3 and PBH4 21.0 kA, PBV1 ± 2.0 kA, PBV2 ± 1.52 kA, PSTR1 and 2 ± 450 A.

II. PERFORMANCE OF THE INJECTION SYSTEM OF THE RCS

The beam injection system of the RCS consists of several DC bending magnets [7], [8] and pulsed bending magnets. The pulsed magnet of the RCS injection system deflects the beam orbit for the painting injection in a transverse plane [9]–[12]. The pulsed magnets are a shift bump magnet (SB) [10], [11], a horizontal painting magnet (PBH) [9], [12], a vertical painting magnet (PBV) [9], [12] and a pulsed steering magnet (PSTR) [13], [14], respectively.

In the steady operation for users, the beam power of 300 kW has been achieved [5]. Furthermore, at the beam injection energy of 181 MeV, the high power beam demonstration of 540 kW was performed in November 2012 [15]. The measured waveforms of the power supply output current of each power supply at the high power beam demonstration are shown in Fig. 1 for the current SB, PBH, PBV and PSTR.

1051-8223 © 2013 IEEE. Personal use is permitted, but republication/redistribution requires IEEE permission.
See http://www.ieee.org/publications_standards/publications/rights/index.html for more information.

Authorized licensed use limited to: Japan Atomic Energy Agency. Downloaded on April 16,2023 at 02:40:11 UTC from IEEE Xplore. Restrictions apply.

III. Specification of the Pulsed Magnets for the Painting Injection in the Transverse Plane

A. Pulsed Magnet for a Fixed Orbit

The four SBs, which are arranged in the RCS injection area, produce a fixed main bump orbit to merge the injection beam from the LINAC into the circulating beam of the RCS. The SBs are connected in series and excited by one power supply. The two PSTRs, which are placed in the injection beam transport line from the LINAC to the RCS (L3BT), switch the injection beam orbit to change the angle at the first charge-exchange foil position [17] at 25 Hz. Each PSTR is excited individually.

B. Pulsed Magnet for a Dynamically Changing Orbit

The four PBHs, which are divided into two pairs, deflect the circulating beam in the horizontal direction. One pair is arranged for the upstream of the SBs, and another pair is arranged on the downstream of the SBs. The two PBVs vary the injection angle vertically at the first charge-exchange foil position. The PBVs are placed in the L3BT line at a betatron phase of π upstream of the stripping foil. Each magnet is excited individually. The PBH and PBV dynamically change the beam orbit using the decaying waveform of the magnet current during the beam injection of 500 μs, which is generated in a square root functions of time [9], [12].

IV. Design of the Pulsed Power Supply for a Fixed Orbit

As for the pulsed power supply of the SBs and PSTRs, the trapezoidal waveform of the magnet current is required. The flat-top of the waveform is used for fixing a beam orbit during the beam injection. In order to form the trapezoidal waveform, a different circuit system of each power supply has been adopted. One is the system with the IGBT chopping and another is the system with the PFN switching capacitor. The IGBT chopping method is used by the injection bump system and the PFN switching capacitor method is used by the PSTR in the present J-PARC RCS. With the energy upgrade of LINAC to 400 MeV, a new power supply of the SB has been designed and manufactured by the PFN switching capacitor method [6], [18].

A. IGBT Chopping System for the Current SB Power Supply

The main circuit of the current SB power supply is composed by the multiplexing circuit of IGBT assemblies, as shown in Fig. 2. One chopper power panel (CHP) is composed by 8 multiplexing circuit of the IGBT assemblies and the circuit is divided on the basis of the midpoint earth (neutral point). Therefore, the voltage applied between magnet terminal and ground can be reduced by half. The carrier frequency of the IGBT element is 6 kHz and the controlled switching frequency is 48 kHz by eight 8 multiplexing circuit of the IGBT assemblies. The power supply output current and output voltage per 1 power panel is 3 kA and 6.4 kV. The constitution of the current SB power supply is 7 parallels (CHP No. is A to G). So the power supply of the current SB excites the maximum current of 21 kA. The performance of the SB power supply has the specification of $\pm 1.0\%$ deviation from the programmed pattern. This specification satisfies the performance of the controlled beam injection orbit with high accuracy and the stability for every shot at the current injection beam energy of 181 MeV.

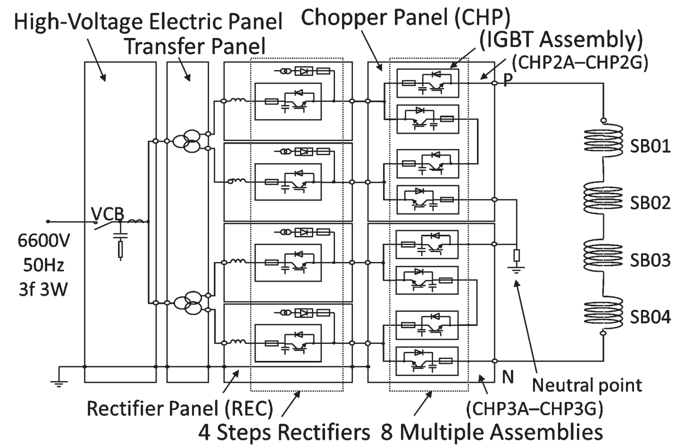

Fig. 2. Schematic view of the main circuit of the current SB power supply.

The power supply generates the required waveform pattern by 48 kHz chopping of the IGBT assemblies. When the output current and falling time are changed, the output voltage is adjusted by monitoring the deviation of the current from the required waveform. The waveform can be changed within the maximum output voltage of 6.4 kV and effective current of 5 kA, of which a rise and a fall time can be changed from 185 μs to 500 μs with the flat-top time to be 620 μs.

B. PFN Switching Capacitor Method for the New SB Power Supply and the PSTR Power Supply

The power supply of the PFN switching capacitor method is composed of the many capacitor banks. The circuit system of the power supply is a commutation strategy using the electrical charge and discharge of the capacitor. The trapezoidal waveform of the power supply output current is created by fewer switching times. The units of the power supply comprise the rise-fall unit and the flat-top unit. The rise-fall unit controls the starting-up and the falling-down processes of the trapezoidal waveform. The flat-top unit keeps the output current constant at the flat-top.

The new SB power supply for the injection energy upgrade has been designed [6], [18], of which the power supply output current is 32 kA and the output voltage is 13.2 kV. The composition of the new SB power supply is 16 banks in parallel. One bank excites the maximum current of 2 kA and the maximum output voltage is 13.2 kV. The schematic view of the one bank is shown in Fig. 3. One bank is composed of 12 rise-fall units and the 2 flat-top units, which are connected in series (positive and negative). The main circuit is divided on the basis of the midpoint earth (neutral point). When a waveform alteration is required, a change of the power supply (PS) voltage and a commutation strategy by the changeover switch is performed at every unit. However, a rise and a fall time cannot be changed individually because the starting-up and the falling-up units are

Authorized licensed use limited to: Japan Atomic Energy Agency. Downloaded on April 16,2023 at 02:40:11 UTC from IEEE Xplore. Restrictions apply.

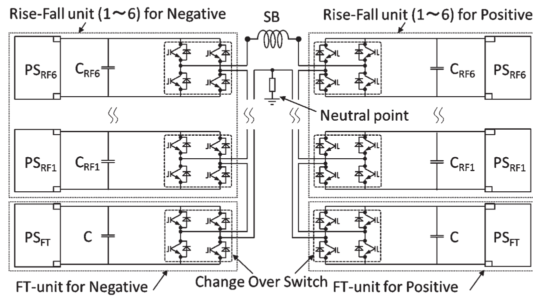

Fig. 3. Schematic view of the main circuit of the new SB power supply with one bank.

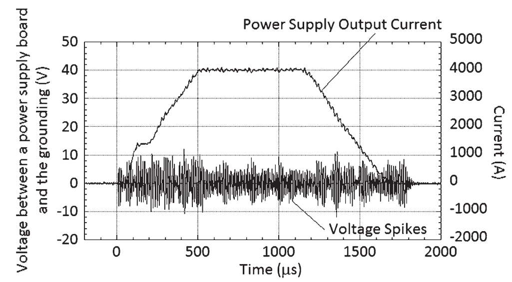

Fig. 4. Measurement result of the power supply output current (upper trace) and the voltage spikes (lower traces) of the current SB with IGBT chopping method.

the same. The fall time can be changed from 150 μs to 500 μs. As for the flat-top time, it is fixed in 650 μs. The power supply of the PSTR excites the maximum current of 450 A and the maximum voltage of 400 V [14]. In the trapezoidal waveform, a rise-fall time is changed from 500 μs to 1500 μs and the flat-top time is changed from 650 μs from 850 μs. The deviation of the output current is $\pm$ 0.2%.

V. Design of the Pulsed Power Supply for a Dynamically Changed Orbit

The power supplies of the PBH and PBV produce the decay waveform pattern of the magnet current. The painting injection controls both the uniformity and the shape of the beam profile by the decay waveform [12], [13]. The decay waveform has a shape of square root function of the injection time, which is produced by the IGBT chopping methods.

The main circuit of the power supply is composed of the multiplexing circuit of IGBT assemblies, which is similar to the current SB power supply. In one chopper power panel, IGBT assemblies are composed of 6 multiples. The phase of the signal carrier is shifted between the positive side and the negative side so that one chopper panels becomes 12 multiples as a whole. The carrier frequency of the IGBT element is 54 kHz. In one chopper power panel, the controlled switching frequency is 648 kHz by 12 multiplexing circuit of the IGBT assemblies. The waveform of the power supply output current is produced by the IGBT chopping with 648 kHz.

VI. Comparison of The IGBT Chopping Method and the PFN Switching Method

One of the causes of the current ripple on the output current waveform is the switching operation of the power source. The induction noise from the stray capacitance between the power supply board and the grounding due to the switching operation causes a potential variation of the power supply. The characteristics of the pulsed power supply with the IGBT choppers and the PFN capacitor switching were obtained by measuring the potential variation. Each potential variation was measured by a voltage probe between the power supply board and the grounding.

The measurement result of the current SB with IGBT chopping method is shown in Fig. 4. And the measurement result of the new SB with PFN switching capacitor method is shown in Fig. 5. In case of the IGBT chopping, the voltage spikes due

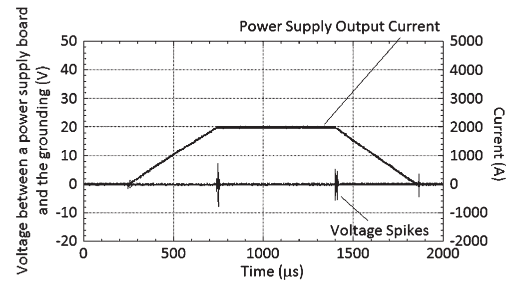

Fig. 5. Measurement result of the power supply output current (upper trace) and the voltage spikes (lower trace) of the new SB with PFN switching capacitor method.

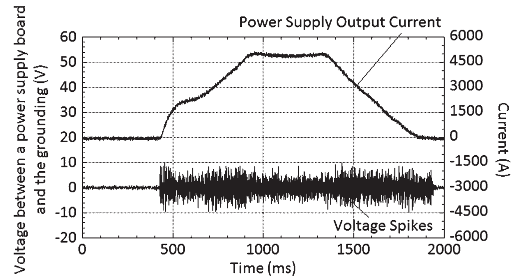

Fig. 6. Measurement result of the trapezoidal waveform with IGBT chopping system of PBH4. Lower trace with voltage spikes shows the potential variation.

to the switching operation were observed throughout all over the power supply output current. In case of the PFN switching, however, the voltage spikes were observed only four times, when the capacitor switching is made to form a trapezoidal waveform.

VII. Influence of the IGBT Chopping Method

The measurement results of the current and voltage spikes for both the trapezoidal waveform and the decay waveform with PBH4, which is produced by the IGBT chopping methods, are shown in Figs. 6 and 7, respectively. In these results, the obvious difference of the waveform pattern is not confirmed. Furthermore, FFT analysis of the measurement results, which are both the power supply output current by PEARSON CT (model 1423) at output point inside the power supply board and the potential voltage with trapezoidal waveform and painting waveform, was performed, are shown in Figs. 8 and 9, respectively. The sampling time of the FFT is about 2 ms. Though the cutoff frequency of the CT is 1.2 MHz, the higher harmonics of

Authorized licensed use limited to: Japan Atomic Energy Agency. Downloaded on April 16,2023 at 02:40:11 UTC from IEEE Xplore. Restrictions apply.

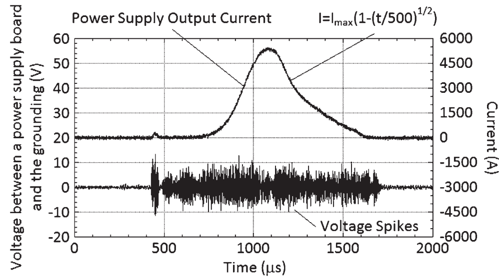

Fig. 7. Measurement result of the painting waveform with IGBT chopping system of PBH4. Lower trace with voltage spikes shows the potential variation.

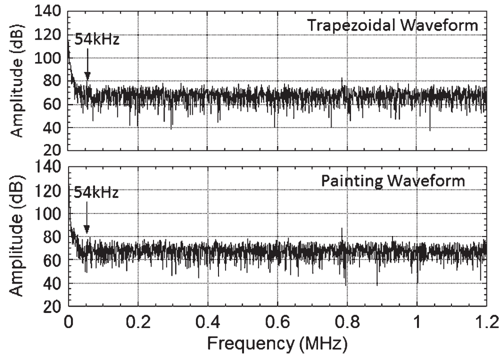

Fig. 8. FFT analysis results of the PEARSON CT with trapezoidal waveform and painting waveform of PBH4.

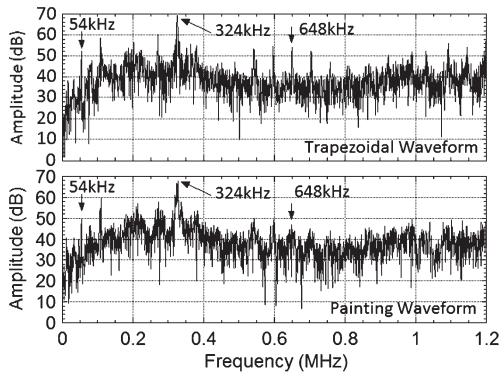

Fig. 9. FFT analysis results of the potential voltage with trapezoidal waveform and painting waveform of PBH4.

over 54 kHz could be seen because of the connection the waveform was observed through a low path filter with 106 kHz cutoff frequency. However, it is confirmed that the switching operation affected the power supply output current. In the FFT analysis of the potential voltage, the peaks were confirmed in the wide range, where the 54 kHz is the IGBT element frequency, the 324 kHz and 648 kHz its higher harmonic components.

The influence upon the beam monitor was obtained by the FFT spectrum of the signal of the H0 dump monitor [17], as shown in Fig. 10. The H0 dump monitor is located at the dump line of the RCS injection area near the PBH4, which monitors the unstripped particles at the charge-exchange foil. The FFT analysis result showed the harmonics components of the IGBT element frequency. The beam signal of the H0 dump monitor is 0.94 MHz and 1.88 MH. The beam monitor is seriously affected by the switching noise with IGBT chopping.

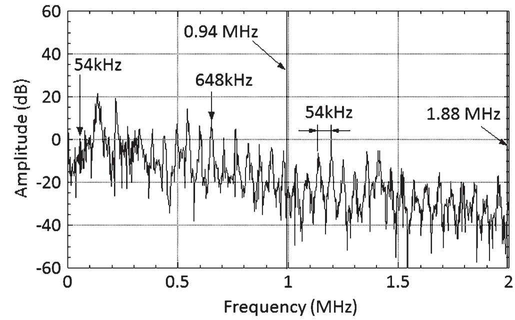

Fig. 10. FFT spectrum of the signal of the H0 dump monitor with PBH4.

VIII. Conclusion

Comparisons of the pulsed power supply system using the IGBT chopping method and the PFN switching capacitor method were performed. As for the PFN system, there was no current ripple in a flat-top time because it switches only in a turning point in order to form the waveform. In case of the IGBT chopping method, the noise is observed continuously over the whole period. However, the IGBT chopping system has the advantage to form an arbitrary waveform pattern. In order to increase the beam intensity for producing 1 MW beam power, not only the reductions of the beam loss due the switching noise but also the painting injection using the arbitrary wave pattern are required. It is in progress to study the reduction of the switching noise due to the IGBT chopping, which improves the phase of the signal carrier and the circuit composition using the multiconductor transmission-line theory [19].

References

[1] "Accelerator technical design report for high-intensity proton accelerator facility project, J-PARC," Japan Atomic Energy Research Institute, Ibaraki, Japan, KEK-Report 2002-13; JAERI-Tech 2003-044, Mar. 2003.

[2] *J-PARC Accelerator*. [Online]. Available: http://j-parc.jp/Acc/en/index.html

[3] K. Hasegwa, M. Kinsho, and H. Oguri, "Status of J-PARC acelerators," in *Proc. IPAC*, 2013, pp. 3830–3832, THPWO031.

[4] M. Kinsho, "Status and progress of the J-PARC 3 GeV RCS," in *Proc. IPAC*, 2013, pp. 3848–3850, THPWO037.

[5] H. Hotchi, M. Kinsho, K. Hasegawa, N. Hayashi, Y. Hikichi, S. Hiroki, J. Kamiya, K. Kanazawa, M. Kawase, F. Noda, M. Nomura, N. Ogiwara, R. Saeki, K. Saha, A. Schnase, Y. Shobuda, T. Shimada, K. Suganuma, H. Suzuki, H. Takahashi, T. Takayanagi, O. Takeda, F. Tamura, N. Tani, T. Togashi, T. Ueno, M. Watanabe, Y. Watanabe, K. Yamamoto, M. Yamamoto, Y. Yamazaki, H. Yoshikawa, and M. Yoshimoto, "Beam commissioning of the 3-GeV rapid cycling synchrotron of the Japan Proton Accelerator Research Complex," *Phys. Rev. ST Accel. Beams*, vol. 12, no. 4, pp. 040402-1–040402-22, Apr. 2009.

[6] T. Takayanagi, N. Hayashi, T. Ueno, T. Togashi, and Y. Irie, "Simulation model for design of a new power supply," *IEEE Trans. Appl. Supercond.*, vol. 22, no. 2, p. 5400704, Jun. 2012.

[7] M. Yoshimoto, J. Kamiya, T. Takayanagi, M. Watanabe, O. Takeda, M. Kinsho, Y. Irie, H. Fujimori, S. Igarasi, and H. Nakayama, "Designs of SEPTUM magnets at 3-GeV RCS in J-PARC," in *Proc. IPAC*, 2006, pp. 1768–1770, WEPD085, TUPLS113.

[8] M. Watanabe, K. Hirano, Y. Irie, J. Kamiya, M. Kinsho, T. Takayanagi, Y. Yamazaki, and M. Yoshimoto, "Injection and extraction DC magnets power supplies for 3GEV rapid cycling synchrotyon OF J-PARC," in *Proc. EPAC*, 2008, pp. 3676–3678, THPP134.

[9] T. Takayanagi, J. Kamiya, M. Watanabe, Y. Yamazaki, Y. Irie, J. Kishiro, I. Sakai, and T. Kawakubo, "Design of the injection bump system of the 3-GeV RCS in J-PARC," *IEEE Trans. Appl. Supercond.*, vol. 16, no. 2, pp. 1358–1361, Jun. 2006.

[10] T. Takayanagi, J. Kamiya, M. Watanabe, T. Ueno, Y. Yamazaki, Y. Irie, J. Kishiro, I. Sakai, T. Kawakubo, S. Tounosu, Y. Chida, M. Watanabe, and

Authorized licensed use limited to: Japan Atomic Energy Agency. Downloaded on April 16,2023 at 02:40:11 UTC from IEEE Xplore. Restrictions apply.

T. Watanuki, “Design of the shift bump magnets for the beam injection of the 3-GeV RCS in J-PARC,” *IEEE Trans. Appl. Supercond.*, vol. 16, no. 2, pp. 1366–1369, Jun. 2006.

[11] T. Takayanagi, K. Kanazawa, T. Ueno, H. Someya, H. Harada, Y. Irie, M. Kinsho, Y. Yamazaki, M. Yoshimoto, J. Kamiya, M. Watanabe, M. Kuramochi, and K. Satou, “Improvement of the shift bump magnetic field for a closed bump orbit of the 3-GeV RCS in J-PARC,” *IEEE Trans. Appl. Supercond.*, vol. 18, no. 2, pp. 306–309, Jun. 2008.

[12] T. Takayanagi, K. Kanazawa, T. Ueno, H. Someya, H. Harada, Y. Irie, M. Kinsho, Y. Yamazaki, M. Yoshimoto, J. Kamiya, M. Watanabe, and M. Kuramochi, “Measurement of the paint magnets for the beam painting injection system in the J-PARC 3-GeV RCS J-PARC,” *IEEE Trans. Appl. Supercond.*, vol. 18, no. 2, pp. 310–313, Jun. 2008.

[13] T. Takayanagi, M. Kinsho, P. Saha, T. Togashi, T. Ueno, M. Watanabe, Y. Yamazaki, M. Yoshimoto, H. Fujimori, and Y. Irie, “Design of the pulse bending magnet for switching the painting area between the MLF and MR in J-PARC 3-GeV RCS,” in *Proc. IPAC*, 2010, pp. 3293–3294, WEPD085.

[14] T. Takayanagi, N. Hayash, K. Horino, M. Kinsho, T. Togashi, T. Ueno, Y. Watanabe, and Y. Irie, “Power supply of the pulse steering magnet for changing the painting area between the MLF and the MR at J-PARC 3 GEV RCS,” in *Proc. IPAC*, 2013, pp. 681–686, MOPWA008.

[15] H. Hotchi, H. Harada, N. Hayashi, M. Kinsho, P. K. Saha, Y. Shobuda, F. Tamura, K. Yamamoto, M. Yamamoto, M. Yoshimoto, Y. Irie, and S. Kato, “High intensity trial of up to 540 kW in J-PARC RCS,” in *Proc. IPAC*, 2013, pp. 3837–3838, THPWO033.

[16] T. Takayangi, N. Hayashi, T. Togashi, T. Ueno, Y. Watanabe, and M. Kinsho, “Upgrade design of the bump system in the J-PARC 3-GeV RCS,” in *Proc. IPAC*, 2011, pp. 3403–3405, THPO028.

[17] P. K. Saha, F. Noda, Y. Irie, H. Hotchi, T. Takayanagi, N. Hayashi, S. Machida, and I. Sakai, “Present design and calculation for the injection-dump line of the RCS at J-PARC,” in *Proc. PAC*, Knoxville, TN, USA, 2005, pp. 3739–3741.

[18] T. Takayanagi, N. Hayashi, T. Ueno, T. Togashi, N. Tani, M. Kinsho, and K. Toda, “New power supply of the injection bump magnet for upgrading the injection energy in the J-PARC 3-GeV RCS,” in *Proc. IPAC*, 2012, pp. 3226–3628, THPPD051.

[19] H. Toki and K. Sato, “Multiconductor transmission-line theory with electromagnetic radiation,” *J. Phys. Soc. Jpn.*, vol. 81, no. 1, pp. 014201-1–014201-12, Jan. 2012.

Authorized licensed use limited to: Japan Atomic Energy Agency. Downloaded on April 16,2023 at 02:40:11 UTC from IEEE Xplore. Restrictions apply.